

**\*\*Volume Title\*\***

*ASP Conference Series, Vol. \*\*Volume Number\*\**

**\*\*Author\*\***

© **\*\*Copyright Year\*\*** *Astronomical Society of the Pacific*

## **A constant characteristic mass for star forming galaxies since $z \sim 3$ revealed by radio emission in the COSMOS field**

Alexander Karim, Eva Schinnerer

*Max-Planck-Institut für Astronomie,  
Königstuhl 17, D-69117 Heidelberg, Germany [email: karim@mpia.de]*

and the VLA-COSMOS & COSMOS collaborations

**Abstract.** We present results of our 1.4 GHz image stacking analysis of mass-selected galaxies in the COSMOS field. From the resulting median radio continuum flux density we have determined the evolution of the average star formation rate (SFR) of galaxies as a function of stellar mass, unbiased from effects of dust but also source confusion due to the 1.5'' angular resolution achieved by the VLA. We find a power-law relation between specific SFR (SSFR) and stellar mass for star forming galaxies out to  $z = 3$ . While higher mass systems exhibit lower SSFRs at any epoch, no differential, more rapid evolution of high mass galaxies is evident at least out to  $z \sim 1.5$  where our conclusions are most robust. Utilizing measured mass functions of star forming systems, the characteristic stellar mass for galaxies contributing most to the comoving SFR density appears not to evolve. These findings hence challenge 'downsizing' scenarios in which star formation has gradually shifted towards lower mass systems with cosmic time. Our analysis constitutes the to-date best determination of the cosmic star formation history (CSFH) since  $z = 3$  and yields indirect evidence for a rapid decline of the global mass density of molecular gas with time.

### **1. Introduction**

A complete census of the global cosmic star formation activity at a given cosmic epoch is usually obtained by measuring/ extrapolating the total star formation rate (SFR) per unit comoving volume. The time evolution of this SFR density (SFRD) is also known as the cosmic star formation history (CSFH). Over the last years several measurements revealed a steep decline of the SFRD since a redshift of  $z \sim 1$  and likely a shallower evolutionary behavior at higher redshifts (see Hopkins & Beacom 2006, for a compilation). Despite the to-date comparatively little observational evidence into the SFRD evolution at high  $z$  – and in particular into the fraction of star formation obscured by dust – it is a widely accepted scenario that the CSFH shows a maximum around  $z = 2 - 3$ .

A number of recent studies revealed a surprisingly tight correlation between the total SFR of normal star forming galaxies and their stellar mass content (e.g. Noeske et al. 2007; Elbaz et al. 2007, for measurements out to  $z \sim 1$ ). The localized process of star formation is consequently linked to a global galaxy property, suggesting that star formation histories of individual galaxies are likely not dominated by stochastic processes such as galaxy mergers (e.g. Noeske et al. 2007). The exact evolutionary properties of this relation are subject to ongoing debates and insights based on a variety of SFR tracers are needed.

Clearly, multi-wavelength look-back surveys are key to reveal how galaxies build up their stellar mass and how their SFRs evolve over a wide range of redshift. The panchromatic datasets from the 2 deg<sup>2</sup> cosmic evolution survey (COSMOS; see Scoville et al. 2007, for an overview), in particular, have provided very accurate photometric redshifts (photo- $z$ s) and stellar masses for a large mass-selected sample of galaxies (Ilbert et al. 2010). In this work we use this Spitzer/IRAC ( $m_{\text{AB}}(3.6 \mu\text{m}) \leq 23.9$ ) selected sample of  $\sim 114,000$  galaxies in combination with high angular resolution Very Large Array (VLA) radio continuum data to measure the evolution of the average SFR as a function of stellar mass out to  $z \sim 3$ . SFRs derived from radio continuum emission require only a simple K-correction and no correction for dust extinction. All methods, results and Figures presented here are discussed in detail in Karim et al. (2011).

## 2. The evolution of the specific star formation rate as a function of stellar mass

Stellar masses have been estimated for all sources via fits of stellar population synthesis models (Bruzual & Charlot 2003, BC03) to the observed spectral energy distributions (SEDs), assuming a Chabrier (2003) initial mass function, exponentially declining star formation histories and a Calzetti et al. (2000) dust extinction law (details on the estimation of stellar masses and photo- $z$ 's are found in Ilbert et al. 2010). From the restframe intrinsic – i.e. dust unextincted –  $(\text{NUV} - r^+)_{\text{temp}} < 3.5$  colors, obtained from the BC03 SED fits, we have separated star forming sources from quiescent ones within our sample.

We have obtained average 1.4 GHz radio flux densities separately for both all and only star forming galaxies from median stacks of cutout images of the VLA-COSMOS map (resolution  $1.5'' \times 1.4''$ ; Schinnerer et al. 2007, 2010) centered at the positions of the  $3.6 \mu\text{m}$  selected sources, after binning each galaxy sample in redshift and mass. We also excluded radio-AGN candidates from the sample – applying various criteria discussed in Karim et al. (2011) – prior to stacking. The resulting total flux densities have been converted into SFRs using the calibration of the radio-infrared correlation in the local universe (Bell 2003).

The average stellar mass normalized SFR (specific SFR/SSFR) is best described by separable power-laws in mass and redshift for both all (massive) galaxies (Fig. 1, left panels) and star forming ones (Fig. 1, right panels). At  $z > 1.5$  the average SSFR of low mass star forming galaxies tends to deviate from the mass-uniform evolutionary trend seen at lower redshifts. There is thus tentative evidence for an upper limit to the average SSFR at just about the inverse of a dynamical timescale of typical local but also higher  $z$  disk galaxies (e.g. Daddi et al. 2010a). While their dynamical and free-fall times are approximately equal, normal galaxies are assumed to accrete their gas from their surroundings and to process it into stars at a constant efficiency (e.g. Daddi et al. 2010b). The upper SSFR-limit we propose might hence represent an effective gas accretion threshold.

## 3. The characteristic mass of star formation

While star forming sources exhibit this remarkably shape-invariant SSFR-mass relation throughout cosmic time in our study, it is worth noting that their stellar mass functions are found to show a similar constancy of their Schechter profile (e.g. Ilbert et al. 2010).

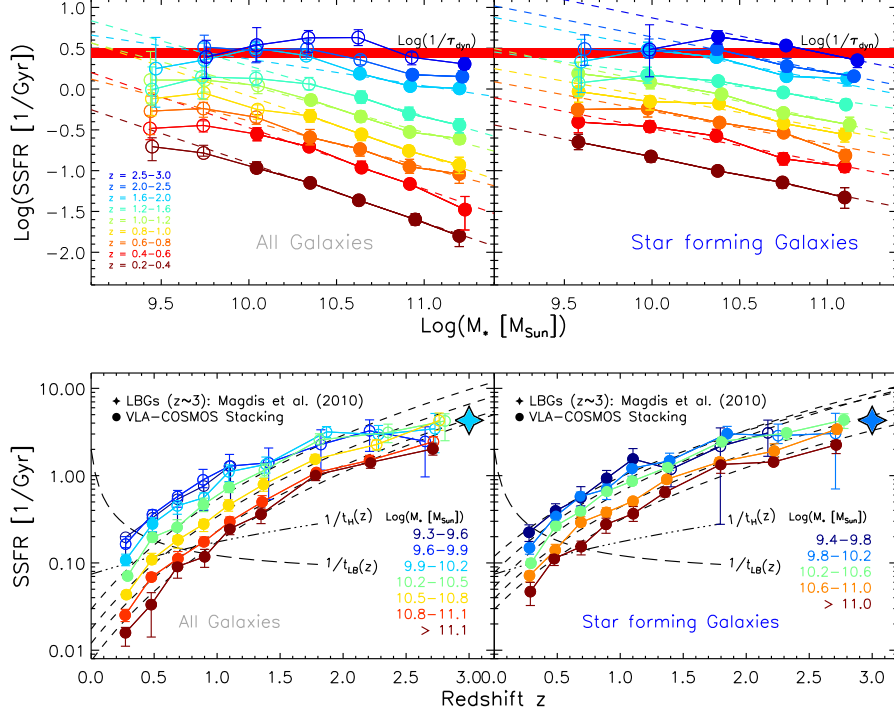


Figure 1. Radio stacking based measurement of the SSFR as a function of stellar mass at  $0.2 < z < 3.0$  (*upper panels*) and redshift evolution of the SSFR in logarithmic stellar mass bins (*lower panels*) for our entire galaxy sample (left) and star forming systems only (right). Full symbols depict samples that are regarded as representative for the underlying galaxy population, open symbols represent upper SSFR limits. For representative data points both the mass dependence of the average SSFR at a given epoch as well as its redshift evolution at fixed mass follow power-laws (dashed lines). Quiescent galaxies (Included in the left panels) are preferentially massive and less frequent at higher  $z$  as seen in (i) deviations from the high-mass end power-law which itself (ii) becomes gradually slightly shallower with redshift. For star forming systems only (right panels) the power-law extends over the entire mass range and all mass-bins evolve uniformly. A separable power-law  $\text{SSFR}(M_*, z) \propto f(M_*) \times g(z) = M_*^{-0.04} \times (1+z)^{3.5}$  hence is a good description for the average SSFR of star forming galaxies at least out to  $z \sim 1.5$ . The horizontal band (*upper panels*) sketches the inverse dynamical timescale, potentially representing an upper bound to the average SSFR (see text) and therefore leading to deviations also for high- $z$  star forming sources. The black long-dashed line gives the mass-doubling limit above which galaxies are able to double their mass until  $z = 0$  assuming a constant SFR. The black dashed-dotted line depicts the inverse age of the universe at any given redshift and hence makes measured SSFRs comparable to the past average star formation activity. The SED-derived measurement of Magdis et al. (2010) for LBGs at  $z \sim 3$  with  $\log(M_*) \sim 10$  is shown as a filled star.

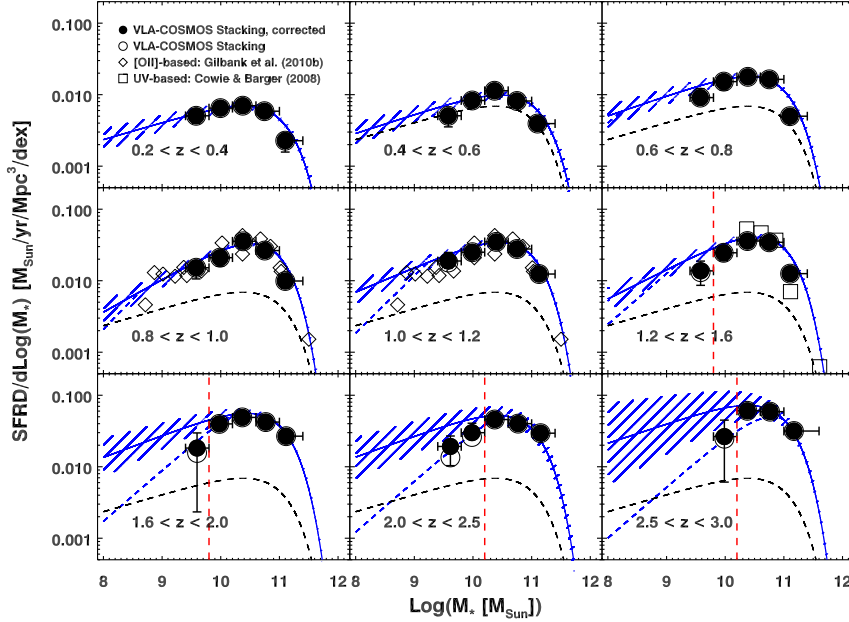


Figure 2. The distribution of the SFRD with respect to stellar mass at different epochs out to  $z \sim 3$ . The data points in each panel are the product of the observed number densities of star forming galaxies with the average (stacking- based) radio SFRs. Leftwards of the dashed vertical lines – in the mass range where our data are not fully representative for the underlying galaxy population – number densities have been corrected using the corresponding mass functions (Ilbert et al. 2010). Uncorrected data are shown as open circles. These corrections are generally small and needed only at  $z > 1.5$ . In each panel we overplot the Schechter function that results from multiplying the best-fit radio derived SFR-mass relation at a given epoch with the corresponding mass function for SF galaxies. Literature results based on the [OII] $\lambda$ 3727 line (Gilbank et al. 2010) as well as UV emission (Cowie & Barger 2008) agree well with the trends in our data. Dashed blue lines show the distribution obtained if an upper limit to the average SSFR at lower masses is assumed.

As both phenomena involve a power-law in stellar mass, the product of the SSFR-mass relation and the mass function at a given cosmic epoch also yields a Schechter function for the mass distribution of the comoving SFR density (SFRD). In Fig. 2 we plot the resulting Schechter SFRD functions along with our direct, radio stacking based, measurements of the SFRD for each bin in mass and redshift and with literature results from alternative SFR diagnostics at different wavelengths. While the potential upper SSFR-limit discussed above might alter the low-mass end shapes significantly only at the highest redshifts, the galaxy mass at which the function peaks at *any* epoch is  $M_* \sim 10^{10.6} M_\odot$ , regardless of the assumption of an SSFR-limit. The existence of this characteristic mass of star forming galaxies challenges a ‘downsizing’ paradigm in which the dominant contributors to the CSFH have been massive sources in the cosmic past and low-mass galaxies at present times. It does, however, not rule out that low-mass sources gain more relative importance over time.

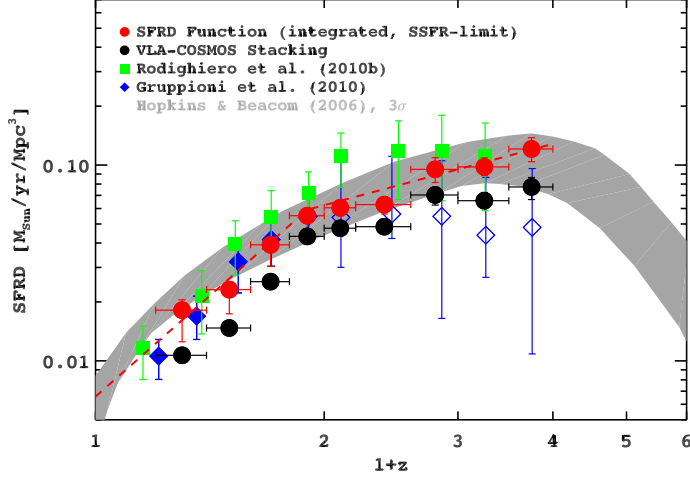


Figure 3. The dust-unbiased CSFH out to  $z = 3$ . Black circles represent the sum of data points the corresponding redshift-bin panel of Fig. 2 and hence a direct – stacking-based – measurement of the SFRD down to the limiting mass at each epoch. Red filled circles correspond to the ‘total’ SFRD at each epoch, obtained by integrating the Schechter-function fit (Fig. 2) down to  $M_* = 10^5 M_\odot$  and assuming an upper limit to the average SSFR. The redshift evolution can be described by a broken power-law (dashed lines) that results from the joint (non-)evolution of the star forming stellar mass density and the evolution of the SFR-mass relation. Recent mid- to far-IR measurements of SFRDs between  $0 < z < 2.5$  (Spitzer/MIPS: Rodighiero et al. 2010; Herschel/PACS: Gruppioni et al. 2010) are shown along with our data and the  $3\sigma$  envelope from the Hopkins & Beacom (2006) compilation. Open symbols denote lower limits. Note the remarkable agreement of the far-IR- and radio-based data at all  $z$ .

#### 4. The dust unbiased cosmic star formation history

The sum of our direct radio stacking based measurements of the SFRD for individual mass bins yields lower limits to the total SFRD at any redshift. At a given redshift the Schechter SFRD function enables us to obtain the remainder of the total SFRD, integrated below our observational mass limits. For this integration we assume the upper bound to the average SSFR motivated above. The resulting radio-based – i.e. dust-extinction unaffected – CSFH out to  $z \sim 3$  is shown in Fig. 3 along with independent literature measurements. Since  $z \sim 1$  the stellar mass density of star forming galaxies is approximately constant (e.g. Ilbert et al. 2010) and also the relative fractions of objects at different masses within this population are conserved due to the shape-invariance of their mass function (see above). In this redshift range the CSFH is therefore entirely controlled by the mass-uniform evolution of the average SFR. Given a constant star formation efficiency, a strong and global decline in the mass density of molecular gas thus entirely explains the observed decrease of the integrated SFRD with cosmic time. Towards earlier epochs it is predominantly the – again mass-uniform – decrease in star forming stellar mass density that leads to a shallower evolutionary behavior. The CSFH since  $z \sim 3$  is hence well described by a broken power-law (Fig. 3).

## 5. Summary and conclusions

Using a median image stacking technique of 1.4 GHz radio continuum emission and an unprecedentedly rich sample of galaxies selected at  $3.6\ \mu\text{m}$  with panchromatic (FUV to mid-IR) ancillary data in the COSMOS field we have measured stellar mass-dependent average (specific) star formation rates ((S)SFRs) in the redshift range  $0.2 < z < 3$ . We have applied various criteria to minimize contaminating radio flux from potential active galactic nuclei and have used the template-based, intrinsic rest-frame  $(\text{NUV} - r^+)_{\text{temp}}$  color from SED-fits in the NUV-mid-IR in order to separate star forming sources from quiescent systems. Our findings – presented in detail in Karim et al. (2011) – are:

- The evolution of the average (S)SFR of stellar mass selected galaxies is approximately mass-independent at least out to  $z \sim 1.5$  where the depth of our data allows the most robust conclusions. A power-law relation between (S)SFR and mass represents well the data at the high mass end.
- The (S)SFR of star forming sources at  $z < 3$  also evolves basically independent of mass while a power-law dependence of (S)SFR and mass generally extends over all masses probed. Higher mass galaxies hence have lower SSFRs, regardless if quiescent galaxies are included in the analysis or not.
- There is tentative evidence for an upper bound to the average SSFR preventing a further growth of the SSFR with  $z$ , starting at the low-mass end at  $z \sim 1.5 - 2$ .
- The stellar mass distribution function of the comoving SFR density at any epoch is well described by a Schechter function that reveals a constant characteristic mass of star formation since  $z \sim 3$ . Its integral yields the total SFRD at any  $z$ .

**Acknowledgments.** We thank A. Martínez-Sansigre, M. Sargent, H.-W. Rix, A. van der Wel, O. Ilbert, V. Smolčić, C. Carilli, M. Pannella, A. Koekemoer, E. Bell and M. Salvato for their numerous contributions to this work.

## References

- Bell, E. F. 2003, *ApJ*, 586, 794  
 Bruzual, G., & Charlot, S. 2003, *MNRAS*, 344, 1000  
 Calzetti, D., et al. 2000, *ApJ*, 533, 682  
 Chabrier, G. 2003, *PASP*, 115, 763  
 Cowie, L. L., & Barger, A. J. 2008, *ApJ*, 686, 72  
 Daddi, E., et al. 2010a, *ApJ*, 714, L118  
 — 2010b, *ApJ*, 713, 686  
 Elbaz, D., et al. 2007, *A&A*, 468, 33  
 Gilbank, D. G., et al. 2010, *MNRAS*, 405, 2419  
 Gruppioni, C., et al. 2010, *A&A*, 518, L27+  
 Hopkins, A. M., & Beacom, J. F. 2006, *ApJ*, 651, 142  
 Ilbert, O., et al. 2010, *ApJ*, 709, 644  
 Karim, A., et al. 2011, *ApJ*, in press. [arXiv:astro-ph/1011.6370](https://arxiv.org/abs/1011.6370)  
 Magdis, G. E., et al. 2010, *ApJ*, 714, 1740  
 Noeske, K. G., et al. 2007, *ApJ*, 660, L43  
 Rodighiero, G., et al. 2010, *A&A*, 515, A8+  
 Schinnerer, E., et al. 2007, *ApJS*, 172, 46  
 — 2010, *ApJS*, 188, 384  
 Scoville, N., et al. 2007, *ApJS*, 172, 1